This article was downloaded by: [Renmin University of China]
On: 13 October 2013, At: 10:28
Publisher: Taylor & Francis
Informa Ltd Registered in England and Wales Registered Number: 1072954 Registered office: Mortimer House, 37-41 Mortimer Street, London W1T 3JH, UK

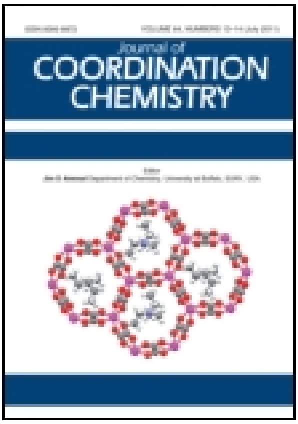

Journal of Coordination Chemistry
Publication details, including instructions for authors and subscription information:
http://www.tandfonline.com/loi/gcoo20

A new organic-inorganic hybrid based on Mn-salen and decavanadate

Shiwei Lin [a b] , Qiong Wu [a c] , Huaqiao Tan [a] & Enbo Wang [a]

[a] Key Laboratory of Polyoxometalate Science of Ministry of Education, Department of Chemistry , Northeast Normal University , 130024 Changchun, P.R. China

[b] Department of Chemistry , Changchun Normal University , 130032 Changchun, P.R. China

[c] Department of Chemistry Science & Technology , Kunming University , 650214 Kunming, P.R. China

Published online: 24 Oct 2011.

To cite this article: Shiwei Lin , Qiong Wu , Huaqiao Tan & Enbo Wang (2011) A new organic-inorganic hybrid based on Mn-salen and decavanadate, Journal of Coordination Chemistry, 64:21, 3661-3669, DOI: 10.1080/00958972.2011.628990

To link to this article: http://dx.doi.org/10.1080/00958972.2011.628990

PLEASE SCROLL DOWN FOR ARTICLE

Taylor & Francis makes every effort to ensure the accuracy of all the information (the "Content") contained in the publications on our platform. However, Taylor & Francis, our agents, and our licensors make no representations or warranties whatsoever as to the accuracy, completeness, or suitability for any purpose of the Content. Any opinions and views expressed in this publication are the opinions and views of the authors, and are not the views of or endorsed by Taylor & Francis. The accuracy of the Content should not be relied upon and should be independently verified with primary sources of information. Taylor and Francis shall not be liable for any losses, actions, claims, proceedings, demands, costs, expenses, damages, and other liabilities whatsoever or howsoever caused arising directly or indirectly in connection with, in relation to or arising out of the use of the Content.

This article may be used for research, teaching, and private study purposes. Any substantial or systematic reproduction, redistribution, reselling, loan, sub-licensing, systematic supply, or distribution in any form to anyone is expressly forbidden. Terms &

Journal of Coordination Chemistry
Vol. 64, No. 21, 10 November 2011, 3661–3669

A new organic–inorganic hybrid based on Mn–salen and decavanadate

SHIWEI LIN†‡, QIONG WU†§, HUAQIAO TAN† and ENBO WANG*†

†Key Laboratory of Polyoxometalate Science of Ministry of Education, Department of Chemistry, Northeast Normal University, 130024 Changchun, P.R. China
‡Department of Chemistry, Changchun Normal University, 130032 Changchun, P.R. China
§Department of Chemistry Science & Technology, Kunming University, 650214 Kunming, P.R. China

(*Received 5 August 2011; in final form 14 September 2011*)

An organic–inorganic hybrid based on Mn-salen and decavanadate, $[NH_4]_2[Mn(salen)(H_2O)_2]_4[V_{10}O_{28}] \cdot 6H_2O$ (**1**) (salen = *N*,*N*′-ethylene-bis(salicylideneiminate)), has been synthesized by the strategy of secondary building units in mixed methanol–water solution and was structurally characterized by single-crystal X-ray diffraction, elemental analyses, IR, and UV-Vis. The $[Mn(salen)(H_2O)_2]^+$ cations and water molecules are located in the interspaces among the polyoxoanions $[V_{10}O_{28}]^{6-}$ forming a POM-based supramolecule. Compound **1** is the first example of metal-Schiff-base polyoxovanadates. The photocatalytic analysis, cyclic voltammetry, and electrocatalytic analysis of **1** have been investigated.

Keywords: Organic-inorganic hybrid; Schiff-base; Salen; Polyoxometalates; Decavanadate

1. Introduction

Design and synthesis of organic–inorganic hybrid compounds are of interest because of their potential applications in catalysis, molecular recognition, absorption, photochemistry, magnetism, medicine, biochemistry, etc. [1]. A strategy is using well-defined organic (or organometallic) and inorganic molecules as secondary building units (SBUs) where distinctive natures will be maintained and synergetic interactions between organic (or organometallic) and inorganic compositions will occur. This strategy provides a rational way to synthesis and fine-tuning of the properties of materials on the molecular level [2]. Polyoxometalates (POMs), as a unique class of inorganic clusters with structural versatility and high negative charges, have been widely employed as inorganic SBUs and a series of POM-based inorganic–organic hybrid materials were obtained [3]. Schiff bases especially those with N_2O_2 donor sets have applications in medicine, catalysis, and magnetic materials [4]. Unfortunately, organic–inorganic

---

*Corresponding author. Email: wangeb889@yahoo.com.cn

Journal of Coordination Chemistry
ISSN 0095-8972 print/ISSN 1029-0389 online
http://dx.doi.org/10.1080/00958972.2011.628990

hybrids based on Schiff bases and POMs determined by single-crystal X-ray diffraction are rare.

We recently initiated an investigation of organic–inorganic hybrids based on metal-Schiff bases and POMs and have prepared some octamolybdate and Anderson-type compounds [5]. As continuation, we isolated $[NH_4]_2[Mn(salen)(H_2O)_2]_4[V_{10}O_{28}] \cdot 6H_2O$ (**1**) (salen = *N*,*N'*-ethylene-bis(salicylideneiminate)). Compound **1** represents the first example of metal-Schiff-base polyoxovanadates.

2. Experimental

2.1. *Materials and methods*

All reagent grade chemicals were purchased and used without purification. The starting materials of salen [6] and $[(C_4H_9)_4N]_3[V_{10}O_{28}H_3]$ [7] were synthesized according to literature methods and characterized by IR spectra. V was analyzed on a PLASMA-SPEC (I) ICP atomic emission spectrometer; C and N analyses were performed on a Perkin-Elmer 2400 CHN elemental analyzer. IR spectra were recorded from 400 to 4000 cm^{-1} on an Alpha Centaurt FT/IR spectrophotometer using KBr pellets. UV-Vis absorption spectrum was obtained using a 752 PC UV-Vis spectrophotometer. Electrochemical measurements were carried out on a CHI 660A electrochemical workstation at 25–30°C under nitrogen. The cell consists of three electrodes: Ag/AgCl(s)/KCl as reference electrode, Pt wire as auxiliary electrode, and glassy C METROHM (diameter = 3 mm) as working electrode.

2.2. *Synthesis*

A mixture of salen and $Mn(CH_3COO)_2 \cdot 4H_2O$ was added into 20 mL of methanol and refluxed for 30 min. The resulting dark brown solution was added into a 20 mL of HAc–NaAc (pH = 4.0) buffer solution containing $[(C_4H_9)_4N]_3[V_{10}O_{28}H_3]$. The mixture was stirred and heated at 75°C for another 30 min. After the solution cooled to room temperature, a small amount of dark brown precipitate was filtered off, and the filtrate was sealed with parafilm containing tiny pores for facilitating slow evaporation at room temperature. Dark brown stick-like crystals of **1** were isolated after 7 days, in 36% yield (based on V) by filtration, washed with methanol, and dried in air. Anal. Calcd for $C_{64}Mn_4V_{10}N_{10}H_{94}O_{50}$ ($M_r = 2532.6$) (**1**) (%): C, 30.35; N, 5.53; Mn, 8.68; V, 20.11. Found (%): C, 30.31; N, 5.58; Mn, 8.64; V, 20.19.

2.3. *X-ray crystallography*

Crystallographic data for **1** were collected at 293 K on a Rigaku R-axis Rapid IP diffractometer using graphite monochromated Mo-Kα radiation ($\lambda = 0.71073$ Å) and IP technique. Multi-scan absorption correction was applied. The crystal data were solved by direct methods and refined by full-matrix least-squares on F^2 using the SHELXTL-97 crystallographic software package [8]. During refinement, all the non-H atoms were anisotropically refined, hydrogen atoms on C and N and POM framework were fixed

Table 1. Crystal data and structure refinement for **1**.

Empirical formula	$C_{64}Mn_4V_{10}N_{10}H_{94}O_{50}$
Formula weight	2532.6
Crystal system	Triclinic
Space group	$P\bar{1}$
Temperature (K)	296(2)
Crystal size (mm^3)	$0.24 \times 0.22 \times 0.18$
λ	0.71073
Unit cell dimensions (Å, °)	
a	13.689(3)
b	13.693(3)
c	13.930(3)
α	62.49(3)
β	79.39(3)
γ	77.53(3)
Volume ($Å^3$), Z	2250.6(8), 0.5
Calculated density ($g\,cm^{-3}$)	1.866
$F(000)$	1264
θ range for data collection (°)	3.02–27.48
Limiting indices	$-12 \le h \le 12$; $-13 \le k \le 13$; $-13 \le l \le 12$
Reflections collected/unique	19,473/4203
R_{int}	0.0678
Data/restraints/parameters	4203/8/324
Completeness (%)	96.7
$R_1(I > 2\sigma(I))$[a]	0.0630
wR_2 (all data)[b]	0.1729
Goodness-of-fit on F^2	1.018

[a] $R_1 = \Sigma[w(F_o^2 - F_c^2)^2/(n - P)]^{1/2}$, where n = number of reflections and p = parameters used.

[b] $wR_2 = \Sigma[w(F_o^2 - F_c^2)^2]/\Sigma[w(F_o^2)^2]^{1/2}$.

on calculated positions, and hydrogen atoms on water were found from the residual peaks and fixed on oxygen with restrained H–O bond distances. Crystal data and structure refinements for **1** are given in table 1. Selected bond lengths and angles of **1** are listed in table 2.

3. Results and discussion

3.1. *Synthesis*

The SUB strategy has been widely employed to obtain organic–inorganic hybrids. Choice of solvent is crucial to such reactions. During the design and synthesis of metal-Schiff base and POMs, we employed buffer solution offering a friendly pH for products; HAc–NaAc (pH = 4.0) buffer solution was chosen for stability of decavanadates during synthesis of **1**. Mixed methanol–water was utilized to increase solubility of the reactants. Parallel experiments showed that the reaction sequence and the temperature of the reaction system are key factors for formation of **1**. It is important to react salen with $Mn(CH_3COO)_2 \cdot 4H_2O$ first; no crystalline product can be obtained if reactants are mixed directly. Suitable heating increases the yield of **1**, but when the temperature is higher than 75°C, no crystalline phase was formed.

Table 2. Selected bond lengths (Å) and angles (°) of **1**.

Mn(1)–O(17)	1.877(5)	Mn(1)–O(20)	1.894(4)
Mn(1)–O(16)	2.246(4)	Mn(1)–O(11)	2.257(5)
Mn(1)–N(1)	1.970(5)	Mn(1)–N(3)	1.974(6)
Mn(2)–O(6)	1.876(5)	Mn(2)–O(21)	1.896(5)
Mn(2)–O(19)	2.241(5)	Mn(2)–O(9)	2.287(5)
Mn(2)–N(4)	1.970(5)	Mn(2)–N(2)	1.987(6)
V(1)–O(4)	1.670(4)	V(1)–O(5)	1.693(4)
V(1)–O(2)	1.871(4)	V(1)–O(3)	2.055(5)
V(1)–O(1)	2.063(4)	V(1)–O(1)#	2.084(4)
V(2)–O(15)	1.598(5)	V(2)–O(13)	1.733(5)
V(2)–O(10)	1.861(5)	V(2)–O(2)	1.980(4)
V(2)–O(3)#	2.124(4)	V(2)–O(1)	2.284(4)
V(3)–O(23)	1.592(5)	V(3)–O(12)	1.781(5)
V(3)–O(7)#	1.819(5)	V(3)–O(2)	2.024(4)
V(3)–O(3)#	2.085(4)	V(3)–O(1)#	2.287(4)
V(4)–O(22)	1.591(5)	V(4)–O(14)#	1.825(5)
V(4)–O(10)#	1.840(5)	V(4)–O(12)	1.918(5)
V(4)–O(5)	2.037(5)	V(4)–O(1)#	2.341(4)
V(5)–O(8)	1.604(5)	V(5)–O(7)	1.821(5)
V(5)–O(14)	1.821(5)	V(5)–O(13)	1.930(5)
V(5)–O(4)	2.065(5)	V(5)–O(1)	2.369(4)
N(1)–Mn(1)–N(3)	82.2(2)	N(3)–Mn(1)–O(16)	89.0(2)
O(20)–Mn(1)–O(11)	92.0(2)	O(16)–Mn(1)–O(11)	177.5(2)
N(4)–Mn(2)–N(2)	81.8(2)	N(4)–Mn(2)–O(9)	91.7(2)
O(6)–Mn(2)–O(9)	86.7(2)	O(19)–Mn(2)–O(9)	176.11(19)
O(4)–V(1)–O(2)	100.8(2)	O(4)–V(1)–O(3)	93.2(2)
O(4)–V(1)–O(1)#	164.5(2)	O(1)–V(1)–O(1)#	77.77(16)
O(15)–V(2)–O(10)	101.8(3)	O(10)–V(2)–O(2)	151.8(2)
O(15)–V(2)–O(1)	172.2(2)	O(3)#–V(2)–O(1)	73.62(15)
O(23)–V(3)–O(12)	105.2(3)	O(12)–V(3)–O(2)	91.3(2)
O(2)–V(3)–O(3)#	73.87(18)	O(23)–V(3)–O(1)#	171.6(2)
O(22)–V(4)–O(12)	101.3(3)	O(14)#–V(4)–O(5)	155.74(19)
O(22)–V(4)–O(1)#	171.9(2)	O(5)–V(4)–O(1)#	72.86(16)
O(8)–V(5)–O(7)	103.4(3)	O(7)–V(5)–O(13)	153.55(19)
O(8)–V(5)–O(1)	171.7(3)	O(4)–V(5)–O(1)	71.39(16)

Symmetry transformations used to generate equivalent atoms: # $-x+1$, $-y+3$, $-z+1$.

3.2. *Crystal structure*

Compound **1** crystallizes in the space group $P\bar{1}$. Compound **1** contains four $[\mathrm{Mn(salen)(H_2O)_2}]^+$, two ammonium atoms, six water molecules, and a decavanadate $[\mathrm{V_{10}O_{28}}]^{6-}$ (figure 1).

In $[\mathrm{Mn(salen)(H_2O)_2}]^+$, the six-coordinated Mn(III) has a distorted octahedral configuration, surrounded by two oxygen atoms and two nitrogen atoms from one salen and two water molecules in axial positions. In the equatorial plane, two Mn–O bond lengths are Mn(1)–O(20) = 1.894(4) Å, Mn(1)–O(17) = 1.877(5) Å with an average of 1.886 Å; the two Mn–N bond lengths are Mn(1)–N(1) = 1.970(5) Å, Mn(1)–N(3) = 1.974(6) Å with an average of 1.972 Å. Axial bond lengths are Mn(1)–O(11) = 2.257(5) Å and Mn(1)–O(16) = 2.246(4) Å with an average of 2.252 Å, slightly longer due to Jahn–Teller distortion at the high-spin d^4 metal center. All Mn centers possess +3 oxidation state based on charge balance considerations [9], as well as Jahn–Teller elongation.

The structure of $[\mathrm{V_{10}O_{28}}]^{6-}$ is built from a packed cluster of 10 distorted $\{\mathrm{VO_6}\}$ octahedra sharing edges. The decavanadates exhibit a cage-like structure made of six

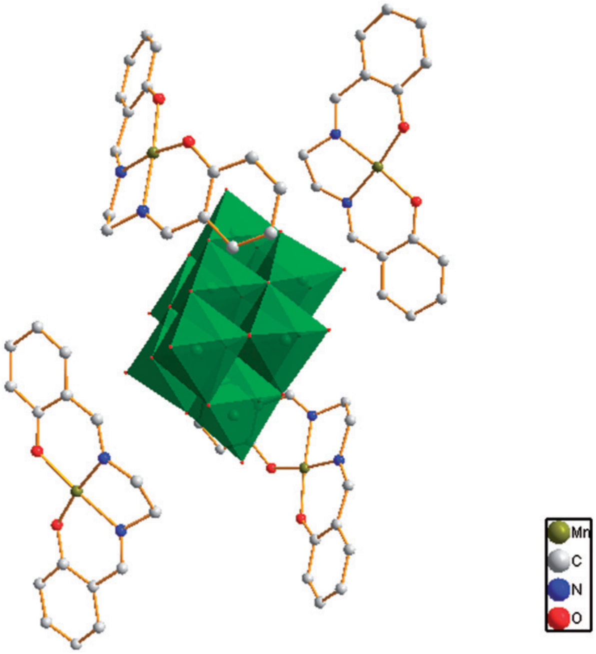

Figure 1. Polyhedral and ball-and-stick representation of **1** with ammonium atoms and water molecules omitted for clarity.

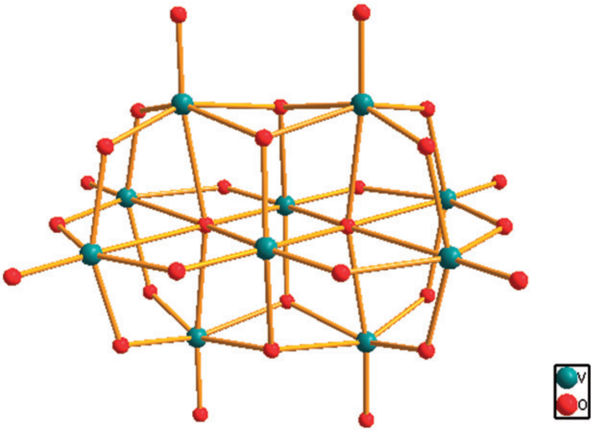

Figure 2. Ball-and-stick representation of the decavanadate anion of **1**.

vanadiums in a plane and four vanadiums above and below the plane (figure 2). Bond parameters associated with the metal centers are comparable with structurally characterized decavanadates [10]. All V–O bond lengths for **1** are listed in table 2. In the asymmetric unit, four terminal V=O bond lengths are in the range 1.591(5)–1.604(5) Å, with an average value of 1.596 Å; each metal of these terminal V=O groups has a very long V–O bond length (2.063(4)–2.369(4) Å) involving hexacoordinated O(1); other V–O bond lengths for these four metal centers are in the range 1.733(5)–2.124(4) Å; remaining V(1) centers without terminal oxo have two short (1.670(4), 1.693(4) Å), two medium (1.871(4), 2.055(5) Å), and two long (2.063(4), 2.084(4) Å) V–O bond lengths.

The $[Mn(salen)(H_2O)_2]^+$ cations and water molecules are located in the interspaces among the polyoxoanions $[V_{10}O_{28}]^{6-}$ forming a POM-based supramolecule as shown in figure 3.

3.3. *IR and UV-Vis spectra*

The IR spectrum (Supplementary material) shows a strong band at 966 cm^{-1} which can be assigned to V=O stretch. Bands at 902, 856, 798, and 732 cm^{-1} correspond to asymmetric bridging V–O–V vibrations. Peaks at 530 and 460 cm^{-1} are Mn–O and Mn–N vibrations, respectively. The ν(C=N) bands of salen are at 1624, 1605, 1531, and 1588 cm^{-1}. Broad bands at 3426 cm^{-1} and a strong peak at 1624 cm^{-1} from O–H

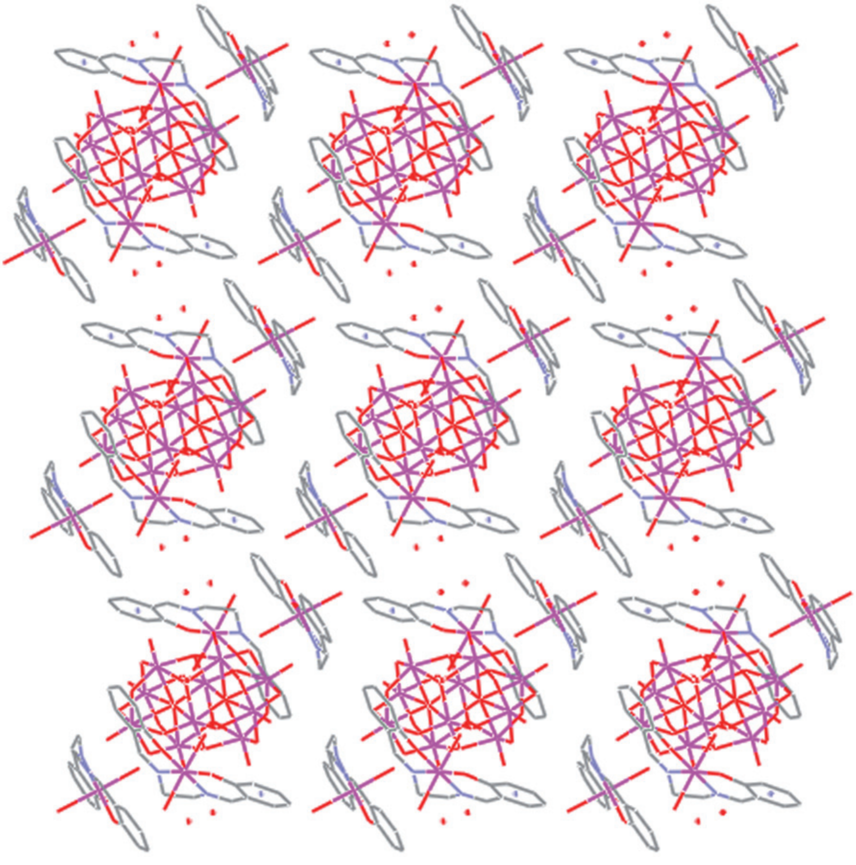

Figure 3. Ball-and-stick view of the 3-D supramolecular framework of **1** along the *b*-axis.

indicate the presence of lattice and coordinated water molecules. Additional bands at 1010–1400 and 2368–3196 cm^{-1} are characteristic for C–N and C–H, N–H, and O–H stretches.

The UV-Vis spectrum of **1** in aqueous solution at $1.0 \times 10^{-3} mol \cdot L^{-1}$ (Supplementary material) has strong peaks at 240 nm and 300 nm attributed to $O \rightarrow V$ ligand-to-metal charge transfer. Absorptions at 356 and 390 nm are ascribed to Mn^{3+} [5b].

3.4. *Photocatalysis property*

POMs possess photocatalytic activities in degradation of organic dyes under UV irradiation by oxidization [11]. We investigated the photocatalytic performances of **1** for photodegradations of RhB with UV irradiation through a typical process: compound **1** ($2.50 \times 10^{-5} mol\, L^{-1}$) and Rhodamine-B (RhB) ($1.40 \times 10^{-5} mol\, L^{-1}$) were dissolved in a HAc/NaAc (pH = 4.0) buffer solution and magnetically stirred in the dark for about 5 min. The solution was then exposed to UV irradiation from 125 W Hg lamp at a distance of 4–5 cm between the liquid surface and the lamp. The solution was kept stirring during irradiations. Every 30 min, 3.0 mL samples were taken out of the beaker for analysis. As shown in figure 4, the absorption of RhB decreased gradually from 0.846 to 0.022 during 6 h. These results suggest that **1** can be used as a potential photocatalyst with activity in reductions of some organic dyes.

3.5. *Electrochemistry*

The electrochemistry of **1** was detected in an Na_2SO_4/H_2SO_4 buffer solution with pH = 2.2, concentration of **1** of $6 \times 10^{-3} mol\, L^{-1}$, and the initial scan direction cathodic. Two redox peaks appear in the potential range 800 to −800 mV (Supplementary

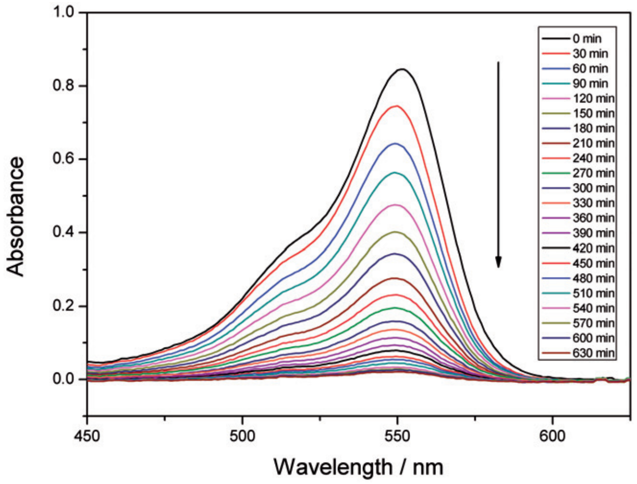

Figure 4. Temporal UV-Vis absorption spectral changes observed for the RhB solutions as a function of irradiation time.

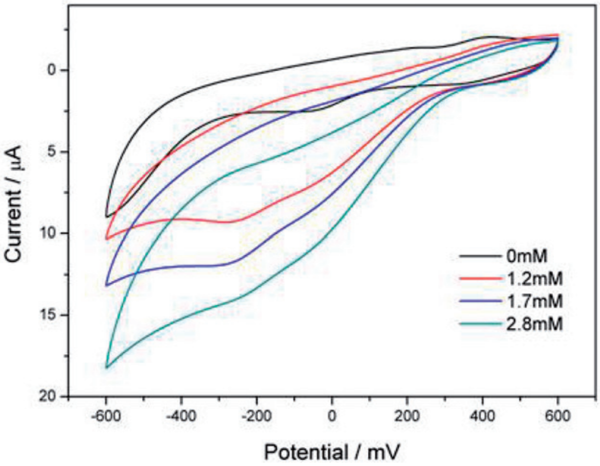

Figure 5. Electrocatalysis of the reduction of BrO_3^- in Na_2SO_4/H_2SO_4 buffer solution with pH = 2.2.

material) ascribed to the electron transfer of the decavanadate. No redox signal of Mn^{3+} is detected in the potential range studied. When the scan rate varies from 20 to 150 mV s^{-1}, the cathodic peak potentials shift to negative and the corresponding anodic peak potentials to positive. Peak-to-peak separations between the corresponding anodic and cathodic peaks increase. Peak currents were proportional to scan rates, suggesting that the redox process of **1** is surface-controlled.

The electrocatalytic properties of **1** were carried out from 0 to −800 mV. Upon addition of modest amounts of bromate, the reduction peak current of II increases while the corresponding oxidation peak current decreases dramatically (figure 5), indicating that **1** displays electrocatalytic activity toward reduction of bromate.

4. Conclusion

A new organic–inorganic hybrid has been prepared *via* reaction between POM units and Mn-Schiff-base complexes. Structural analyses show that **1** represents the first metal-Schiff-based polyoxovanadate characterized by single-crystal X-ray diffraction. This research provides a promising route for design and synthesis of inorganic–organic hybrid materials based on POMs and metal-Schiff bases. Further research on the reactions between different POM units and various metal-Schiff base complexes is ongoing to obtain new metal-Schiff-based POM complexes.

Supplementary material

Crystallographic data for the structural analysis of **1** have been deposited with the Cambridge Crystallographic Data Center with CCDC reference number 835753.

The data can be obtained free of charge at www.ccdc.cam.ac.uk/conts/retrieving.html, or from the Cambridge Crystallographic Data Centre, 12 Union Road, Cambridge CB2 1EZ, UK (Fax: +44-1223-336-033; E-mail: deposit@ccdc.cam.ac.uk).

Acknowledgments

This work was supported by the National Natural Science Foundation of China (No. 20701005/20701006); the Science and Technology Development Project Foundation of Jilin Province (No. 20060420); the Postdoctoral station Foundation of Ministry of Education (No. 20060200002); the Testing Foundation of Northeast Normal University; the Program for Changjiang Scholars and Innovative Research Team in University; and the Natural Science Foundation of Changchun Normal University.

References

[1] (a) P.J. Hagrman, D. Hagrman, J. Zubieta. *Angew. Chem. Int. Ed.*, **38**, 2638 (1999); (b) D. Loy, K. Shea. *Chem. Rev.*, **95**, 1431 (1995); (c) A.P. Wight, M.E. Davis. *Chem. Rev.*, **102**, 3589 (2002); (d) C.R. Kagan, D.B. Mitzi, C.D. Dimitrakopoulos. *Science*, **286**, 945 (1999).

[2] (a) N.L. Rosi, J. Eckert, M. Eddaoudi, D.T. Vodak, J. Kim, M. O'Keeffe, O.M. Yaghi. *Science*, **300**, 1127 (2003); (b) G. FIrey, C. Mellot-Draznieks, C. Serre, F. Millange, J. Dutour, S. Surbli, I. Margiolaki. *Science*, **309**, 2040 (2005); (c) P.Y. Feng, X.H. Bu, N.F. Zheng. *Acc. Chem. Res.*, **38**, 293 (2005).

[3] (a) X.L. Wang, C. Qin, E.B. Wang, Z.M. Su, Y.G. Li, L. Xu. *Angew. Chem. Int. Ed.*, **45**, 7411 (2006); (b) K. Wassermann, M.H. Dickman, M.T. Pope. *Angew. Chem. Int. Ed.*, **36**, 1445 (1997); (c) T. Liu, Y.J. Zhang, Z.M. Wang, S. Gao. *J. Am. Chem. Soc.*, **130**, 10500 (2008); (d) A. Müller, S.Q.N. Shah, H. Bögge, M. Schmidtmann. *Nature*, **397**, 48 (1999); (e) Q. Wu, Y.G. Li, Y.H. Wang, E.B. Wang, Z.M. Zhang, R. Clérac. *Inorg. Chem.*, **48**, 1606 (2009); (f) J.M. Breen, W. Schmitt. *Angew. Chem., Int. Ed.*, **47**, 6904 (2008).

[4] (a) M. Hitoshi, C. Rodolphe, W. Wolfgang, L. Lollita, B. Claire, S. Ken-ichi, Y. Masahiro. *Angew. Chem. Int. Ed.*, **43**, 2801 (2004); (b) K.C. Gupta, A.K. Sutar. *Coord. Chem. Rev.*, **252**, 1420 (2008); (c) H. Miyasaka, A. Saitoh, S. Abe. *Coord. Chem. Rev.*, **251**, 2622 (2007); (d) W. Radecka-Paryzek, V. Patroniak, J. Lisowski. *Coord. Chem. Rev.*, **249**, 2156 (2005); (e) P. Cozzi. *Chem. Soc. Rev.*, **33**, 410 (2004); (f) F. Bedioui. *Coord. Chem. Rev.*, **144**, 39 (1995); (g) M. Sigman, E. Jacobsen. *J. Am. Chem. Soc.*, **120**, 4901 (1998).

[5] (a) Q. Wu, Y.G. Li, Y.H. Wang, R. Clérac, Y. Lu, E.B. Wang. *Chem. Commun.*, 5743 (2009); (b) Q. Wu, W.L. Chen, D. Liu, C. Liang, Y.G. Li, S.W. Lin, E.B. Wang. *Dalton Trans.*, **40**, 56 (2011); (c) Y.W. Li, Y.H. Wang, Y.G. Li, E.B. Wang. *Inorg. Chem. Commun.*, **12**, 112 (2009).

[6] L.J. Boucher. *J. Inorg. Nucl. Chem.*, **36**, 531 (1974).

[7] G. Hervé, A. Tézé. *Inorg. Synth.*, **27**, 83 (1990).

[8] G.M. Sheldrick. *SHELXL-97, Program for Crystal Structure Refinement*, University of Göttingen, Göttingen, Germany (1997); G.M. Sheldrick. *SHELXS97, Program for Crystal Structure Solution*, University of Göttingen, Göttingen, Germany (1997).

[9] I.D. Brown, D. Altermatt. *Acta Crystallogr., Sect. B: Struct. Sci.*, **B41**, 244 (1985).

[10] (a) V.W. Day, W.G. Klemperer, D.J. Maltbie. *J. Am. Chem. Soc.*, **109**, 2991 (1987); (b) D.C. Crans, M. Mahroof-Tahir, O.P. Anderson, M.M. Miller. *Inorg. Chem.*, **33**, 5586 (1994); (c) P. Román, A. Aranzabe, A. Luque, J.M. Gutiérrez-Zorrilla, M. Martínez-Ripoll. *Dalton Trans.*, **20**, 2225 (1995).

[11] (a) W.L. Chen, B.W. Chen, H.Q. Tan, Y.G. Li, Y.H. Wang, E.B. Wang. *J. Solid State Chem.*, **183**, 310 (2010); (b) Y.H. Guo, Y.H. Wang, C.W. Hu, Y.H. Wang, E.B. Wang, Y.C. Zhou, S.H. Feng. *Chem. Mater.*, **12**, 3501 (2000); (c) C. Chen, W. Zhao, P. Lei, J. Zhao, N. Serpone. *Chem. Eur. J. Chemistry*, **10**, 1956 (2004); (d) T. Wu, G. Liu, J. Zhao, H. Hidaka, N. Serpone. *J. Phys. Chem. B*, **103**, 4862 (1999).